The Journal of Chemical Physics

Inertial effects of self-propelled particles: From active Brownian to active Langevin motion

Cite as: J. Chem. Phys. **152**, 040901 (2020); https://doi.org/10.1063/1.5134455
Submitted: 30 October 2019 . Accepted: 15 December 2019 . Published Online: 22 January 2020

Hartmut Löwen

The Journal of Chemical Physics PERSPECTIVE scitation.org/journal/jcp

Inertial effects of self-propelled particles: From active Brownian to active Langevin motion

Cite as: J. Chem. Phys. 152, 040901 (2020); doi: 10.1063/1.5134455
Submitted: 30 October 2019 • Accepted: 15 December 2019 •
Published Online: 22 January 2020

Hartmut Löwen[a)]

AFFILIATIONS

Institut für Theoretische Physik II: Weiche Materie, Heinrich-Heine-Universität Düsseldorf, D-40225 Düsseldorf, Germany

[a)]hlowen@hhu.de

ABSTRACT

Active particles that are self-propelled by converting energy into mechanical motion represent an expanding research realm in physics and chemistry. For micrometer-sized particles moving in a liquid ("microswimmers"), most of the basic features have been described by using the model of overdamped active Brownian motion. However, for macroscopic particles or microparticles moving in a gas, inertial effects become relevant such that the dynamics is underdamped. Therefore, recently, active particles with inertia have been described by extending the active Brownian motion model to active Langevin dynamics that include inertia. In this perspective article, recent developments of active particles with inertia ("microflyers," "hoppers," or "runners") are summarized both for single particle properties and for collective effects of many particles. These include inertial delay effects between particle velocity and self-propulsion direction, tuning of the long-time self-diffusion by the moment of inertia, effects of fictitious forces in noninertial frames, and the influence of inertia on motility-induced phase separation. Possible future developments and perspectives are also proposed and discussed.

I. INTRODUCTION

The dynamics of self-propelled particles that are perpetually moving by converting energy ("fuel") into mechanical motion represent a nonequilibrium phenomenon. Research in the last decades was not only driven by the broad range of applications (such as precision surgery, drug delivery, and cargo transport on the micrometer-scale) but also from a more fundamental level in terms of identifying basic relevant models to describe the particle trajectories under nonequilibrium conditions. One of the first standard models in this respect is the Vicsek model of flocking proposed in 1995 by Vicsek and co-workers,[1] which is by now a cornerstone in describing collective active matter systems. With the upsurge of synthetic colloidal Janus-like particles that create their own gradient in which they are moving, artificial microswimmers were considered as model systems for active matter. These micrometer-sized particles typically self-propel in a liquid at a very low Reynolds number. Therefore, the dynamics of these colloidal particles in a solvent is overdamped, and one of the most popular descriptions is obtained by *active Brownian motion*[2–4] combining solvent kicks described as Gaussian white noise and overdamped motion together with an effective self-propulsion force representing the particle self-propulsion. The active Brownian particle model has been tested against experimental data of self-propelled colloids[2,5,6] and has been used also to describe and predict collective phenomena for colloids and bacteria.[7]

More recently, there have been developments to consider larger self-propelled particles or motion in low-density environment (gas instead of liquid). Then, the motion is no longer at a low Reynolds number. Instead, inertial effects are getting relevant in the dynamics and need to be included in the modeling. These inertia-dominated particles are "microflyers" or "hoppers," "runners" rather than "microswimmers," since their dynamics is underdamped and corresponds to flying rather than swimming. Still the motion is affected by fluctuating random kicks of the surrounding medium. Correspondingly, one can coin their dynamics as *active Langevin motion* rather

than active Brownian motion. However, it is remarked here that sometimes in the literature,[8,9] the term "active Brownian motion" is used in a more general sense including also underdamped Langevin equations of motion.

Examples are mesoscopic dust particles in plasmas (so-called "complex plasma").[10] Pairs of such dust particles can be brought into a joint self-propulsion[11] by nonreciprocal interactions induced by ionic wake charges.[12] These motions are only virtually damped. Another important realization is constituted by granulars made self-propelling on a vibrating plate[13–22] or equipped with an internal vibration motor[23] where it has been shown that the active Langevin model indeed describes their dynamics well.[24–26] Further examples for self-propelled particles with inertia range from minirobots[27,28] and macroscopic swimmers (see Ref. 29 for a recent review) to beetles flying[30] or swimming[31] at water interfaces and whirling fruits self-propelling in air.[32]

In this perspective article, we first briefly review basic features and predictions of active Brownian motion discussing both swimmers moving on average on a straight line ("linear" or equivalently "achiral," "left-right symmetric" swimmers) and particles swimming on a circle ("circle" or "chiral" swimmers). Both single particle properties and collective effects such as motility-induced phase separation (MIPS) are briefly discussed. We then extend the model toward active Langevin motion including inertia and summarize recent developments. We show that some of the basic properties of active Brownian motion are qualitatively changed due to inertia. In particular, we discuss inertial delay effects between particle velocity and self-propulsion direction, the tuning of the long-time self-diffusion by the moment of inertia, effect of fictitious forces in noninertial frames, and the influence of inertia on motility-induced phase separation (MIPS). MIPS is strongly influenced and suppressed by inertia and if there are two coexisting phases of high and low particle density, these coexisting phases possess different kinetic temperatures.

This paper is organized as follows: In Sec. II, we first recapitulate the basic features of active Brownian motion both for linear swimmers and for circle swimmers. Then, in Sec. III, we propose and discuss the model of active Langevin motion. Section IV summarizes the behavior of translational and orientational autocorrelation functions. In Sec. V, experimental realizations of active Langevin motion are described and possible perspectives of future research are discussed in Sec. VI. Finally, we conclude in Sec. VII.

II. ACTIVE BROWNIAN MOTION FOR SELF-PROPELLED COLLOIDAL PARTICLES ("MICROSWIMMERS")

Let us first recapitulate the basic features for overdamped active Brownian motion. In the xy-plane, a single particle trajectory at time t is described by the particle center $\vec{r}(t) = (x(t), y(t))$ and particle orientation $\hat{n}(t) = (\cos\phi(t), \sin\phi(t))$, where $\phi(t)$ is the angle of the particle orientation with the x-axis. We now distinguish between linear swimmers and circle swimmers, which experience a systematic torque.

A. Linear swimmers

For a linear swimmer, the basic overdamped equations of motion read as

$$\gamma\dot{\vec{r}}(t) = \gamma v_0\hat{n}(t) + \vec{f}(t), \tag{1}$$

$$\gamma_R\dot{\phi}(t) = g(t). \tag{2}$$

These equations couple translational and rotational motion and represent a force and torque balance. In detail, γ denotes a translational friction coefficient, v_0 is the imposed self-propulsion speed of the active particle, and γ_R is a rotational friction coefficient. The components of $\vec{f}(t)$ and $g(t)$ are Gaussian random numbers with zero mean and variances representing white noise from the surrounding, i.e., $\overline{\vec{f}(t)} = 0$, $\overline{f_i(t)f_j(t')} = 2k_BT\gamma\delta_{ij}\delta(t-t')$, $\overline{g(t)} = 0$, $\overline{g(t)g(t')} = 2k_BT_R\gamma_R\delta(t-t')$, where the overbar means a noise average. Here, k_BT denotes an effective thermal energy quantifying the translational noise strength. Likewise, k_BT_R characterizes the orientational noise strength. We can thereby define a translational diffusion constant

$$D_t = k_BT/\gamma \tag{3}$$

and a rotational diffusion constant

$$D_r = k_BT_R/\gamma_R. \tag{4}$$

In many applications, the temperatures are set to be equal, i.e., $T \equiv T_R$; in others, the translational noise is neglected with respect to the rotational noise such that $T = 0$ and $T_R > 0$. In the noise-free case $T = T_R = 0$, the self-propelled motion is linear along the particle orientation, i.e., the self-propelled particle is a *linear (or achiral) swimmer*. Its propulsion speed is the imposed v_0. As a remark, the orientational dynamics (2) can equivalently be written as

$$\gamma_R\dot{\hat{n}}(t) = \vec{g}(t)\times\hat{n}(t), \tag{5}$$

where we extended all vectors to three dimensions such that $\hat{n} = (n_x, n_y, 0)$ and $\vec{g}(t) = (0, 0, g(t))$.

Let us first discuss the number of independent parameters inherent to the equations of motion (1) and (2). By choosing suitable units for length and time such as the persistence length

$$\ell_p = v_0/D_r \tag{6}$$

and the persistence time

$$\tau_p = 1/D_r, \tag{7}$$

scaling of the equations results in

$$\frac{d\vec{\tilde{r}}}{d\tilde{t}} = \hat{\tilde{n}}(t) + \sqrt{\frac{2D_t\tau_p}{\ell_p^2}}\vec{\tilde{f}}(\tilde{t}), \tag{8}$$

$$\frac{d\tilde{\phi}}{d\tilde{t}} = \sqrt{2}\tilde{g}(\tilde{t}) \tag{9}$$

with the dimensionless time $\tilde{t} = t/\tau_p$ and the scaled dimensionless functions $\vec{\tilde{r}}(\tilde{t}) = \vec{r}(t)/\ell_p$, $\tilde{\phi}(\tilde{t}) = \phi(t)$, $\hat{\tilde{n}} = (\cos\tilde{\phi}, \sin\tilde{\phi})$ and Gaussian white noises $\vec{\tilde{f}}(\tilde{t})$, $\tilde{g}(\tilde{t})$ of unit variance. Hence, there is only one remaining independent parameter, which can be chosen to be a dimensionless *translational diffusivity*

$$\tilde{D} = D_t/(\ell_p^2/\tau_p) = \frac{k_B T}{\gamma v_0^2 \tau_p}. \tag{10}$$

The number $\tilde{D}$ measures the strength of the bare translational diffusion characterized by the short-time diffusion constant D_t relative to the diffusion generated by the persistent random walk, ℓ_p^2/τ_p. For $\tilde{D} \ll 1$, pure translational diffusion can be neglected. In fact, for $\tilde{D} = 0$ (or equivalently $T = 0$), the model set by Eqs. (1) and (2) is a completely parameter-free persistent random walk solely characterized by the persistence length and persistence time, which is indeed frequently assumed in studies on active Brownian motion. Conversely, in the much less considered case $\tilde{D} \gg 1$, activity is dominated by translational diffusion.

We now address the noise-averaged displacement as a function of time t for a prescribed initial orientation $\hat{n}(0)$ at time $t = 0$. It is given by[2,4,33]

$$\overline{\vec{r}(t) - \vec{r}(0)} = \frac{v_0}{D_r}(1 - e^{-D_r t})\hat{n}(0) = \ell_p(1 - e^{-t/\tau_p})\hat{n}(0). \tag{11}$$

This represents a linear segment oriented along $\hat{n}(0)$ whose total length for $t \to \infty$ is the persistence length ℓ_p. The intuitive interpretation of Eq. (11) is that due to the coupling between translational and rotational motion, the trajectories show a persistence; it is a persistent random walk rather than a standard random walk. The particle remembers where it came from since it is self-propelled along its orientation and the orientation diffuses with D_r. It is the orientational fluctuations that are governing the persistence, not the translational fluctuations. The motion is, therefore, a "random drive" rather than a "random walk": A blind driver steers a car with fluctuations in the steering wheel orientation, and this is what makes the motion persistent.

Next, we can calculate the mean-square displacement (MSD), which is analytically given by[2,4]

$$\overline{(\vec{r}(t) - \vec{r}(0))^2} = 2\ell_p^2\left(\frac{t}{\tau_p} - 1 + \exp\left(-\frac{t}{\tau_p}\right)\right) + 4D_t t. \tag{12}$$

Of course, the MSD does not depend on the initial orientation $\hat{n}(0)$ due to rotational symmetry. Expanding Eq. (12) for small, intermediate, and long times, we obtain a diffusive short-time limit for the MSD as $4D_t t$ for $t/\tau_p \ll \tilde{D}$. For $\tilde{D} \ll 1$, the initial diffusive regime is then followed by a ballistic regime at intermediate times set by $\tilde{D} \ll t/\tau_p \ll 1$, where the MSD scales as $(v_0 t)^2$. For long times, $t/\tau_p \gg 1$, the MSD is again diffusive as $4D_L t$ but with a larger long-time diffusion coefficient given by

$$D_L = \lim_{t\to\infty} \frac{1}{4t}\overline{\vec{r}(t) - \vec{r}(0)}^2 = D_t + v_0^2\tau_p/2 = \frac{\ell_p^2}{\tau_p}\left(\tilde{D} + \frac{1}{2}\right). \tag{13}$$

Remarkably, for strong self-propulsion, $\tilde{D} \ll 1$, D_L is much larger than D_t such that $D_L = \ell_p^2/\tau_p$ is consistent with the persistent random walk picture.

It is important to note that in the overdamped Brownian model, the velocities $\dot{\vec{r}}(t)$ are not real observables as they fluctuate without any bounds due to the noise terms in Eq. (1). Instead, one can define an averaged or drift velocity by $\vec{v}_d(t) = \lim_{\Delta t\to 0}\overline{(\vec{r}(t+\Delta t) - \vec{r}(t))}/\Delta t$, which is given by $\vec{v}_d(t) = v_0\hat{n}(t)$, i.e., the systematic part of the particle drift velocity is the self-propulsion velocity. However, still one can define a velocity autocorrelation function $Z(t)$ as a second time-derivative of the mean-square displacement,[34,35]

$$Z(t) = \frac{d^2}{dt^2}\overline{(\vec{r}(t) - \vec{r}(0))^2}. \tag{14}$$

In the case of active Brownian motion, Eq. (12) yields that the velocity autocorrelation function is a *single exponential*

$$Z(t) = v_0^2 \exp\left(-\frac{t}{\tau_p}\right), \tag{15}$$

decaying with the persistence time τ_p. This result also implies that the mean squared velocity is the self-propulsion speed as given by the short-time limit $Z(0) = v_0^2$.

Remarkably, the orientational correlation function $C(t)$ is also a *single exponential*

$$C(t) = \overline{\hat{n}(t)\cdot\hat{n}(0)} = \exp\left(-\frac{t}{\tau_p}\right), \tag{16}$$

decaying with the same persistence time τ_p, i.e., it is proportional to $Z(t)$. This documents that we have standard Brownian orientational diffusion in two dimensions.[36]

Moreover, one finds for the dynamical correlation function between particle orientation and the drift velocity,

$$\begin{aligned} c(t', t) &:= \lim_{\Delta t\to 0}\overline{\hat{n}(t')\cdot(\vec{r}(t+\Delta t) - \vec{r}(t))/\Delta t} \\ &= v_0 \exp\left(-\frac{1}{\tau_p}|t - t'|\right) \end{aligned} \tag{17}$$

and, finally, a delay function that measures how the dynamical changes of orientation and velocities are correlated can be defined via

$$d(t) = c(t, 0) - c(0, t) \equiv 0. \tag{18}$$

The delay function trivially vanishes here by symmetry, but this will not hold for inertia as discussed later.

Experimental data for the noise averages obtained for dilute self-propelled colloidal Janus particles could indeed be described with these predictions[33,37] establishing that active Brownian motion is the basic model for active colloidal particles.

B. Circle swimmers

In practice, microswimmers are not perfectly rotationally symmetric around their swimming axis. An asymmetry leads to a systematic circular or chiral motion. In two spatial dimensions, this has been described by including an effective torque M in the equations of motion[38] as

$$\gamma\dot{\vec{r}}(t) = \gamma v_0\hat{n}(t) + \vec{f}(t), \tag{19}$$

$$\gamma_R\dot{\phi}(t) = M + g(t). \tag{20}$$

Now, the noise-free trajectories are circles with a spinning frequency

$$\omega_s = \frac{M}{\gamma_R} \tag{21}$$

and a spinning radius

$$R_s = \frac{v_0 \gamma_R}{M}. \tag{22}$$

The sign of the torque M determines whether the circling motion is clockwise or anticlockwise. Compared to Eqs. (1) and (2), there is an additional independent system parameter, which can be chosen as an additional reduced time scale related to the spinning frequency

$$\omega_s \tau_p = \frac{M}{\gamma_R} \tau_p. \tag{23}$$

Again, the mean displacement can be calculated analytically and turns out to be a logarithmic spiral ("*spira mirabilis*") given by[38]

$$\overline{\vec{r}(t) - \vec{r}(0)} = \frac{\ell_p}{1 + (\omega_s \tau_p)^2} \Big[\hat{n}(0) + \omega_s \tau_p \hat{u}(0) - e^{-t/\tau_p} (\hat{n}(t) + \omega_s \tau_p \hat{u}(t)) \Big] \tag{24}$$

with

$$\hat{n}(t) = (\cos(\omega_s t + \phi(0)), \sin(\omega_s t + \phi(0))) \text{ and}$$
$$\hat{u}(t) = (-\sin(\omega_s t + \phi(0)), \cos(\omega_s t + \phi(0))).$$

Likewise, the MSD for circle swimmers is obtained as[38]

$$\overline{(\vec{r}(t) - \vec{r}(0))^2} = \frac{2\ell_p^2}{(1 + (\omega_s \tau_p)^2)^2} \Big[(\omega_s \tau_p)^2 - 1 + (1 + (\omega_s \tau_p)^2) \frac{t}{\tau_p} + e^{-t/\tau_p} [(1 - (\omega_s \tau_p)^2) \cos(\omega_s t) - 2\omega_s \tau_p \sin(\omega_s t)] \Big] + 4 D_t t, \tag{25}$$

which is diffusive for both short times and long times with the short-time diffusion coefficient D_t and the long-time diffusion coefficient

$$D_L = D_t + \frac{v_0^2 \tau_p}{2} \frac{1}{1 + (\omega_s \tau_p)^2}, \tag{26}$$

which implies that circular spinning will reduce the long-time diffusion coefficient relative to Eq. (13).

From Eq. (14), the velocity autocorrelation function can be calculated as

$$Z(t) = v_0^2 \cos(\omega_s t) \exp(-\frac{t}{\tau_p}). \tag{27}$$

It is not a single exponential but contains a further time scale $1/\omega_s$ reflecting the systematic spinning of the particle orientation.

Finally, the orientational correlation function is

$$C(t) = \overline{\hat{n}(t) \cdot \hat{n}(0)} = \cos(\omega_s t) \exp(-\frac{t}{\tau_p}). \tag{28}$$

It is proportional to $Z(t)$ and contains the further time scale $1/\omega_s$ of particle circling as well.

For anisotropic colloidal self-propelled Janus particles, the active Brownian model was tested in detail in experiments. In particular, the *spira mirabilis* for the mean displacement was confirmed.[5]

Finally, we note that the active Brownian motion model of a single particle can be generalized to the presence of external potentials (such as confinement or gravity) and external flow fields (such as linear shear flow) for a review of the different situations considered (see Ref. 7).

C. Collective effects of active Brownian particles: MIPS

Active Brownian particles exhibit a wealth of fascinating collective effects including flocking,[1] vortices,[39] network formation,[40] synchronization,[41] clustering,[7,42] crystallization,[43–46] and turbulence.[47] Here, we focus more on one important effect that is purely induced by activity and is called motility-induced phase separation (MIPS). It was seen in computer simulations of active Brownian particles without aligning interactions[48,49] and confirmed in experiments on artificial colloidal Janus-particles.[49,50]

The basic idea behind MIPS is as follows: Consider a system of active Brownian particles at a finite concentration where the particles are interacting by purely repulsive nonaligning interactions. Suppose two particles meet in a perfect central collision as sketched in Fig. 1(a). Due to the opposed self-propulsion, they will not bounce back but stay close to each other. This is in stark contrast to equilibrium where repulsive force will separate the particle pair immediately. The particles can only get split by fluctuations; in fact, rotational diffusion will turn the orientations away such that they can pass along each other. This process will happen on a time scale of $\tau_p = 1/D_r$. If other particles will approach the particle pair within this time, the pair will be surrounded by more particles, a cluster is formed, and it will get increasingly difficult to release the particles from the cluster. The cluster is thus growing and ideally there is complete phase separation into a dense region inside the cluster and a dilute (depleted) region outside. Clearly, the travel time from a neighboring particle to the initial pair is governed by the particle motility v_0; hence, the particle phase separation is purely induced by motility and is, therefore, called motility-induced phase separation

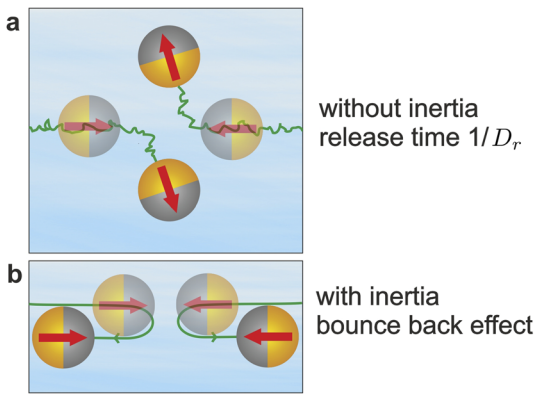

FIG. 1. Sketch of a central elastic collision of two Janus particles with opposing self-propulsion velocities (red arrow). (a) Active Brownian dynamics: the particles will stay almost touching for a typical time of $1/D_r$. (b) Active Langevin dynamics: microflyers will bounce back such that they will not exhibit their terminal self-propulsion speed v_0. Initial positions are shown in light colors. The particle trajectories are rendered in green.

(MIPS). Conversely, in equilibrium (i.e., without motility at $v_0 = 0$), purely repulsive interactions will never lead to liquid-gas phase separation. Based on this intuitive picture, MIPS needs a finite activity to happen and is also favored by higher particle densities since the particles are closer anyway. Both trends are confirmed in simulations (see, e.g., Refs. 51–54) and in a thermodynamic theory (see, e.g., Ref. 55–57). In a parameter space spanned by the particle density and the self-propulsion velocity v_0, there is either a one-phase or a two-phase region. This is by now well-explored by simulation, theory, and experiment, and there are several reviews on this topic.[7,42,58–61]

More recently, MIPS has also been seen for circle swimmers[62,63] (see also Refs. 64 and 65). As found in Ref. 62, an increasing torque acting on circle swimmers hinders MIPS as particles are rotating away from the aggregated clusters. Moreover, more complicated aligning interactions were considered and MIPS was found as well.[66–68] This shows that the occurrence of MIPS itself is a very robust and general effect. Moreover, the growth exponent of the cluster size as a function of time has been simulated[69] and studied by theory.[70] At the late stage, for long times, a universal power law with a universal growth exponent of 1/3 was found similar to the traditional Cahn-Hilliard theory.

III. ACTIVE LANGEVIN MOTION FOR SELF-PROPELLED PARTICLES WITH INERTIA ("MICROFLYERS")

A. Single particles

We now generalize the equations of active Brownian to that of active Langevin motion including inertia both for the translational and the rotational part (see, e.g., Refs. 23, 26, and 71–80) as

$$\begin{aligned} m\ddot{\vec{r}}(t) + \gamma\dot{\vec{r}}(t) &= \gamma v_0 \hat{n}(t) + \vec{f}(t), \\ J\ddot{\phi}(t) + \gamma_R\dot{\phi}(t) &= M + g(t). \end{aligned} \tag{29}$$

Here, m is the particle mass and J the moment of inertia. For $M = 0$, we recover active Langevin motion for linear microflyers, and for $M \neq 0$, these are circle flyers. Now, the particle velocity and the orientation are not necessarily collinear.

On top of the parameters characterizing a Brownian circle swimmer discussed in Sec. II B, there are now two more system parameters. These can be best put in terms of two additional relaxation time scales due to the finite moment of inertia and mass. The *orientational relaxation time* upon which an angular velocity relaxes due to the finite moment of inertia is given by

$$\tau_r = J/\gamma_R. \tag{30}$$

In case the orientational relaxation is fast, $\tau_r \to 0$, one may consider the limit of vanishing moment of inertia, $J = 0$, which was assumed in several recent studies.[72–74,77] Conversely, the case $J \neq 0$, but $m = 0$ has also been considered in the literature.[81] Correspondingly, there is also a second time, the *translational relaxation time*,

$$\tau = m/\gamma, \tag{31}$$

upon which the translational velocities relax due to the finite mass m.

With suitable basic length and time scales of the persistence random walk, ℓ_p and τ_p, we can state the four independent system parameters of Eq. (29) as three basic dimensionless *delay numbers* $\mathcal{D}_0 = \tau_r/\tau_p$, $\mathcal{D}_1 = \omega_s\tau_r$, and $\mathcal{D}_2 = \tau_r/\tau$ plus the dimensionless translational diffusivity $\tilde{D}$ defined in Eq. (10), which contributes a time scale from the translational Brownian motion.

Some analytical solutions of the active Langevin motion model are given in Ref. 26, which we briefly review here. For more analytical results, see Ref. 82. Four different regimes can be identified where the MSD exhibits different power laws: ballistic for very short times, then diffusive due to solvent noise, then ballistic again due to self-propulsion, and then diffusive again for very long times due to randomizing particle orientation. The long-time translational self-diffusion coefficient D_L can be calculated as

$$D_\mathrm{L} = D_t + \frac{v_0^2\tau_p}{2}\mathcal{G}(\mathcal{D}_0, \mathcal{D}_1). \tag{32}$$

This equation has a similar structure than the result for overdamped dynamics [see Eq. (26)], as it is a superposition of the translational diffusion and an active term proportional to $v_0^2\tau_p$. The corresponding dimensionless correction is given by

$$\mathcal{G}(\mathcal{D}_0, \mathcal{D}_1) = \mathcal{D}_0 e^{\mathcal{D}_0}\mathrm{Re}\Big[\mathcal{D}_0^{-(\mathcal{D}_0 - i\mathcal{D}_1)}\gamma(\mathcal{D}_0 - i\mathcal{D}_1, \mathcal{D}_0)\Big], \tag{33}$$

where Re denotes the real part and $\gamma(y, z)$ is the lower incomplete gamma function. Interestingly, the dimensionless correction (33) does *not* depend on the translational relaxation time τ, but it depends explicitly on the rotational relaxation time τ_r (via $\mathcal{D}_0$). This is in contrast to equilibrium ($v_0 = 0$) where D_L depends neither on τ nor on τ_r. In fact, the dependence of long-time diffusion on the moment of inertia J is pretty strong, and it increases with J documenting the additional persistence with larger J. For small J, one obtains

$$D_\mathrm{L} = D_t + \frac{v_0^2}{2D_r} + \frac{v_0^2}{2\gamma_R}J + \mathcal{O}(J^2), \tag{34}$$

while for large J, the asymptotics is governed by

$$D_\mathrm{L} = D_t + v_0^2\sqrt{\frac{\pi}{8D_\mathrm{r}\gamma_R}}\sqrt{J} + \mathcal{O}\Big(\sqrt{J^{-1}}\Big). \tag{35}$$

As an application, animals can hardly change mass, but they can change their moment of inertia during motion. So increasing J may provide a strategy to sample space more quickly.

Moreover, the zero-time velocity correlation, i.e., the mean kinetic energy, can be calculated as

$$Z(0) = 2D_t/\tau + \mathcal{F}(\mathcal{D}_0, \mathcal{D}_1, \mathcal{D}_2)v_0^2 \tag{36}$$

with the dimensionless function

$$\mathcal{F}(\mathcal{D}_0, \mathcal{D}_1, \mathcal{D}_2) = \mathcal{D}_2 e^{\mathcal{D}_0}\mathrm{Re}\Big[\mathcal{D}_0^{-(\mathcal{D}_0 - i\mathcal{D}_1 + \mathcal{D}_2)}\gamma(\mathcal{D}_0 - i\mathcal{D}_1 + \mathcal{D}_2, \mathcal{D}_0)\Big]. \tag{37}$$

The first term in (36) is the equilibrium solution for a passive particle ($v_0 = 0$) and the second arises from the active motion. Similar to (27), the latter is proportional to v_0^2, i.e., the kinetic energy injected by the propulsion.

Remarkably, the orientational correlation function $C(t) = \overline{\hat{n}(t)\cdot\hat{n}(0)}$ is a *double exponential*[81]

$$C(t) = \cos(\omega_s t)\ \exp\left(-D_r\left(t - \tau_r\left(1 - e^{-t/\tau_r}\right)\right)\right), \tag{38}$$

emphasizing again the important role of rotational inertial relaxation since the time scale τ_r enters here explicitly.

Finally, we consider the delay function $d(t)$ (18) that measures how the dynamical changes of orientation and velocities are correlated. One finds

$$\begin{aligned} d(t) &= c(t,0) - c(0,t) = \overline{\dot{\vec{r}}(t)\cdot\hat{n}(0)} - \overline{\dot{\vec{r}}(0)\cdot\hat{n}(t)} \\ &= v_0\mathcal{D}_2 e^{\mathcal{D}_0}\mathcal{D}_0^{(\mathcal{D}_2-\mathcal{D}_0)} e^{-t/\tau}\mathrm{Re}\Big[\mathcal{D}_0^{i\mathcal{D}_1}\Big(\mathcal{D}_0^{-2\mathcal{D}_2}\gamma(\mathcal{D}_0 - i\mathcal{D}_1 + \mathcal{D}_2, \mathcal{D}_0) \\ &\quad - e^{2t/\tau}\mathcal{D}_0^{-2\mathcal{D}_2}\gamma\Big(\mathcal{D}_0 - i\mathcal{D}_1 + \mathcal{D}_2, \mathcal{D}_0 e^{-t/\tau_r}\Big) \\ &\quad - \gamma\Big(\mathcal{D}_0 - i\mathcal{D}_1 - \mathcal{D}_2, \mathcal{D}_0 e^{-t/\tau_r}\Big) + \gamma(\mathcal{D}_0 - i\mathcal{D}_1 - \mathcal{D}_2, \mathcal{D}_0)\Big)\Big]. \end{aligned} \tag{39}$$

By definition, this function is zero for $t = 0$. For linear microflyers, it is then strictly positive, exhibiting a maximum after a typical characteristic delay time. This shows that on average, first the particle orientation will change and then the particle velocity will follow on the scale of this "velocity-orientation delay time." Expression (39) implies that the velocity-orientation decay time depends in a complicated way on τ_r, τ, $1/\omega_s$, and τ_p.

We close this section with two remarks: First, for $J = 0$, there is an equivalence to overdamped particle motion in a harmonic potential as can easily be seen by replacing the role of velocities and positions in the equations of motion. This mapping has led to some other exact results for the dynamics obtained by Malakar and co-workers.[83]

Second, in addition to the mean-square displacements, higher-order moments such as the non-Gaussian parameter, the moment-generating function, or the full probability density provide more general spatiotemporal information about the dynamical behavior of active agents. Using various methods, these quantities have been addressed for the active-Brownian particle model[4,6,37,84] and for the Brownian circle swimmer[85] but not yet for active Langevin particles. As documented in Refs. 26 and 82, such a calculation is, in principle, possible but tedious.

Third, there are more complicated models to describe an additional alignment between particle orientation and velocity, which is ignored in Eq. (29). An extra term involves an additional torque such that the orientational dynamics in Eq. (29) can be written for $J = 0$ as

$$\gamma_R\dot{\hat{n}}(t) = \zeta(\hat{n}(t)\times\dot{\vec{r}}(t))\times\hat{n}(t) + (\vec{M} + \vec{g}(t))\times\hat{n}(t), \tag{40}$$

where ζ is a coupling coefficient. (40) seems to be a more realistic description of granular hoppers[14,23,86] but lacks an analytical solution. It has been applied to describe inertial active particles in a harmonic external potential recently.[23]

B. Self-propulsion of microflyers in noninertial frames

The equations of motion [Eq. (29)] can be generalized to noninertial frames to describe self-propulsion on rotating disks or on oscillating plates, for example, as has been discussed recently.[87] The new phenomenon for active Langevin motion in this setup is that additional fictitious forces have to be added to the equations of motion if the equations are expressed in the noninertial frame. We briefly illustrate this for a planar rotating disk and for an oscillating plate.

1. Rotating disk

On a planar disk rotating around the z-axis with a constant angular velocity ω, the equations of motion for a particle self-propelling on the xy-plane read in the laboratory frame as

$$\begin{aligned} m\ddot{\vec{r}}(t) + \gamma(\dot{\vec{r}}(t) - \vec{\omega}\times\vec{r}(t)) &= \gamma v_0\hat{n}(t) + \vec{f}(t), \\ J\ddot{\phi}(t) + \gamma_R(\dot{\phi}(t) - \omega) &= M + g(t). \end{aligned} \tag{41}$$

The ingredient here is that friction is proportional to the *relative* velocity and the *relative* angular velocity in the rotating noninertial frame. If expressed as equations of motion in the rotating frame, the friction term is getting easier but additional centrifugal and Coriolis forces need to be included.

In the noise-free case, the solution can be found analytically and is given by a superposition of three terms: two logarithmic spirals that spiral inwards and outwards with different rates and a constant rotation around the rotation origin with radius

$$b = \frac{\gamma v_0}{\sqrt{m^2(\omega+\omega_s)^4 + \gamma^2\omega_s^2}}. \tag{42}$$

The special circular solution can be understood as arising from a balance of the centrifugal force, the self-propulsion force, and the friction force in the rotating frame. However, it is unstable with respect to the out-spiraling part, which stems from the action of the centrifugal force. The actual trajectories look pretty complex in the laboratory frame. An example is shown in Fig. 2. For an overdamped system, these fictitious forces do not exist and a particle does not suffer from the centrifugal expulsion from the rotation center.

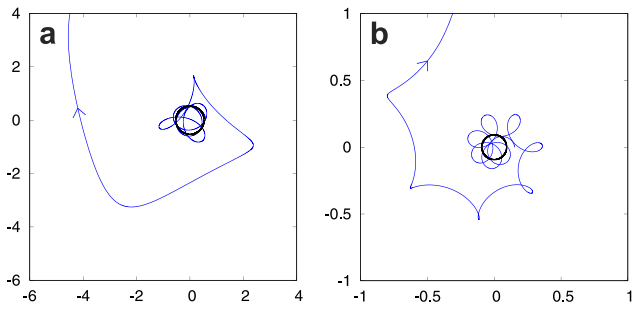

FIG. 2. Typical trajectories from the analytical solution of the noise-free equation (41) in the laboratory frame. The unstable rotation with radius b is indicated as a black circle. The trajectory approaches a logarithmic spiral. The length unit is v_0/ω, and the parameters are as follows: $\gamma/m\omega = 2.5$. (a) $\omega_s/\omega = 1$ and (b) $\omega_s/\omega = 4$.

2. Oscillating plate

We now consider active Langevin motion on a two-dimensional oscillating plate. The oscillating plate constitutes a linearly accelerated frame of reference as described with a time dependent distance vector

$$\vec{R}_0(t) = D_p \cos(\omega_p t)\vec{e}_x \tag{43}$$

between the origins of the inertial laboratory frame and the noninertial frame. Here, D_p is an oscillation amplitude, ω_p is the oscillation frequency of the plate, and the oscillation is taken along the x-axis without loss of generality. The equations of motion in the laboratory frame are

$$m\ddot{\vec{r}}(t) + \gamma(\dot{\vec{r}}(t) - \dot{\vec{R}}_0(t)) = \gamma v_0 \hat{n}(t) + \vec{f}(t), \tag{44}$$

$$\gamma_R \dot{\phi}(t) = M + g(t), \tag{45}$$

and the solution in the noise-free case can be obtained analytically as a superposition of harmonic terms with frequencies ω_p and M/γ_R in the x-direction. One term is exponentially damped with rate γ/m, and another is persistent and undamped. The effect of noise, the noise-averaged trajectory, and the MSD can be calculated analytically following the analysis proposed in Ref. 87. For large ω_p (i.e., $\omega_p \gg M/\gamma_R$), there is an enormous amplification of the oscillation amplitude due to the fictitious inertial force.

C. Collective effects: MIPS

Since motility-induced phase separation (MIPS) is, in general, a pretty robust effect, it is expected to occur also for inertial active particles, provided that the inertial effects are not too large. In fact, recent studies[88,89] have explored the active Langevin model in this regard and found that inertia as modeled by the many-body generalization of Eq. (29) is unfavorable for MIPS. An example is shown in Fig. 3 where the phase separation separatrix is shown for fixed density in the parameter space spanned by the self-propulsion velocity v_0 and the particle mass m. In this case, the moment of inertia J and the external torque M were both set to zero and $T = T_R$. In fact, beyond a critical mass, there is no phase separation at all. Generally speaking, this has to do with the additional fluctuations, which occur in the active system introduced by inertia. If we take the intuitive picture for MIPS in underdamped systems described in Sec. II C, it is now getting different: with inertia, a centrally colliding particle pair will *bounce back* rather than staying static and Brownian as it does in the overdamped case [see Fig. 1(b)]. This will destroy the nucleus for subsequent particle aggregation more than it does in the overdamped case, and therefore, MIPS is unfavored by inertia. Moreover, there is a re-entrant one-phase region if the activity (or self-propulsion) is increased, which is strongly amplified by inertia.

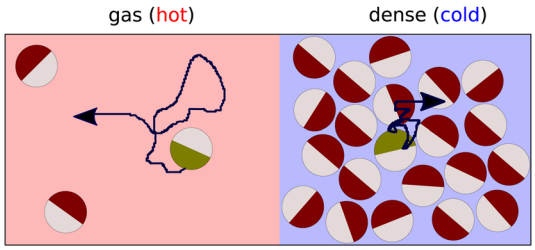

FIG. 4. Scheme of the phase-separated state associated with a hot-cold coexistence in underdamped active particles. Particles self-propel with the colored cap ahead (brown; greenish for the tagged particle). Active particles move with v_0 in the gas phase but can be an order of magnitude slower in the dense phase due to multiple collisions. Reproduced with permission from Mandal *et al.*, Phys. Rev. Lett. **123**, 228001 (2019). Copyright 2019 American Physical Society.

However, when MIPS occurs for inertial active particles, there is a novel effect that does not occur for overdamped systems: the two coexisting phases exhibit a different kinetic temperature.[89,90] Here, temperature is defined via the mean kinetic energy of the particles. Figure 4 shows the underlying principle. In contrast to granulars where a similar effect has been found,[91] particle collisions are elastic here, but the self-propulsion makes a collision between two particles like two bouncing balls hitting each other [see Fig. 1(b)]. Thus, particles will never possess a velocity along their orientation when there are many subsequent interparticle collisions. Therefore, the dense region is "cool" (in terms of kinetic temperature), while in the dilute region, particles will accelerate until they have almost reached their terminal velocity v_0. Hence, the dilute region is "hot." The

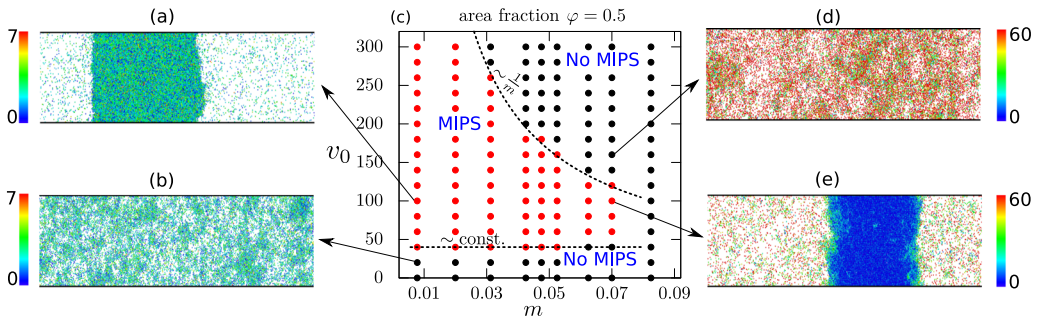

FIG. 3. Nonequilibrium phase diagram at an area fraction of $\varphi = 0.5$ in the plane spanned by the particle mass and the self-propulsion speed (arbitrary units) (c). Panels (a), (b), (d), and (e) represent simulation snapshots in slab geometry at state points indicated in the phase diagram. Colors represent kinetic energies of individual particles in units of k_BT. A hot-cold coexistence is visible in panel (e). Dashed lines in (c) show scaling predictions for the phase boundary between the homogeneous and phase-separated state. Reproduced with permission from Mandal *et al.*, Phys. Rev. Lett. **123**, 228001 (2019). Copyright 2019 American Physical Society.

temperature difference between the dilute and dense regions can be huge up to a factor of 100. Note that there is no flux of heat at the fluid-fluid interface, but a stable thermal gradient will be self-sustained there.

Finally, the growth of particle clusters during the phase separation process has been explored by computer simulation.[89] These calculations reveal that the cluster growth exponent is significantly lower than the universal value of 1/3 found in the overdamped case,[69,70] proving that inertia can qualitatively change the physics of the collective phenomena.

In summary, in the active Langevin model, there are three basic effects, which are caused by inertia as far as motility-induced phase separation is concerned: the phase separation is shifted toward higher Peclet numbers and is finally destroyed completely as the particle mass is increased. Second, the kinetic temperature is different in the two coexisting phases in stark contrast to equilibrium thermodynamics where phase coexistence implies equality of temperatures. Third, the cluster growth exponent is smaller than the universal value 1/3 valid for overdamped systems.

As an outlook, for chiral active Langevin particles, once they exhibit MIPS, one will expect that there are four different temperatures in the two coexisting states (as opposed to a single one in equilibrium coexistence): two different rotational and two different translational ones.

IV. SUMMARY OF TRANSLATIONAL AND ORIENTATIONAL DYNAMICAL AUTOCORRELATION FUNCTIONS

In Table I, we summarize the different cases discussed so far in terms of the translational and orientational dynamical autocorrelation functions $Z(t)$ and $C(t)$. We distinguish between a simple single exponential decay with one decay time and more complicated behavior such as an oscillatory decay (valid for circle swimmers) or double exponentials (valid for microflyers with $M = 0$ and $J > 0$). The passive cases are listed as references, too. For passive Langevin dynamics,

$$m\ddot{\vec{r}}(t) + \gamma\dot{\vec{r}}(t) = \vec{f}(t) \tag{46}$$

with $\vec{f}(t)$ denoting Gaussian white noise, the velocity autocorrelation function $Z(t)$ decays as a simple exponential with a decay time m/γ, and the orientational dynamics is decoupled from this equation. For $J = 0$ and $M = 0$, the orientational correlation is single exponential, but not for $J > 0$ where it is a double exponential or for $M > 0$ where it is oscillatory.

For many particles with nonaligning interactions (at vanishing external torque, $M = 0$), the orientational correlation function is still a single exponential, but the translational correlation function is highly nontrivial (even for passive particles[34]), while for aligning interactions, the orientational dynamics is also complicated.[36]

V. EXPERIMENTAL REALIZATION

A. General

Inertial effects are getting relevant, in particular, for two different situations: (i) for *macroscopic* self-propelled particles and (ii) for mesoscopic particles on the colloidal scale moving in a medium of *low viscosity* (such as a gas).

Regarding the first situation, one of the best realization of our model equations (29) for active Langevin dynamics can be found for active granulars.[13–22] Typically, these are hoppers with a broken fore-aft symmetry, e.g., by tilted legs. In order to achieve self-propulsion, these macroscopic bodies are either placed on a vibrating table or equipped with an internal vibration motor ("hexbugs").[23] It has been shown that the dynamics of these hoppers are well described by active Brownian motion with inertia.[24–26] Since they are macroscopic, inertia is relevant. The fluctuations can be fitted to Brownian forces, and imperfections in the particle symmetry will make them circling ($M \neq 0$). Therefore, they are ideal realizations of our model equations (29), but there is a caveat for certain granulars insofar

TABLE I. Summary of the behavior of translational and orientational correlation functions $Z(t)$ and $C(t)$ for different situations of single and many passive and active particles. The relevant associated time scales are also included. In particular, a simple single exponential decay is indicated. All four different combinations do occur, and the models belonging to the corresponding classes are listed. The notation . . . means that there are more time scales arising from the interparticle interaction.

	Translational velocity correlation $Z(t)$			Orientational correlation $C(t)$		
Single particle	Single exponential	More complicated	Time scales	Single exponential	More complicated	Time scales
Passive Brownian motion	No correlation		. . .	X		τ_p
Active Brownian motion	X		τ_p	X		τ_p
Brownian circle swimmer		X	τ_p, $1/\omega_s$		X	τ_p, $1/\omega_s$
Passive Langevin ($J = M = 0$)	X		τ	X		τ_p
Passive Langevin ($J > 0$ or $M > 0$)	X		τ		X	τ_p, τ_r or $1/\omega_s$
Active Langevin ($M = J = 0$)		X	τ, τ_p	X		τ_p
Active Langevin ($J \neq 0$)		X	τ, τ_p, $1/\omega_s$, τ_r		X	τ_p, $1/\omega_s$, τ_r
Many interacting particles						
Nonaligning ($M = 0$)		X	. . .	X		τ_p
Aligning interaction		X	. . .		X	. . .

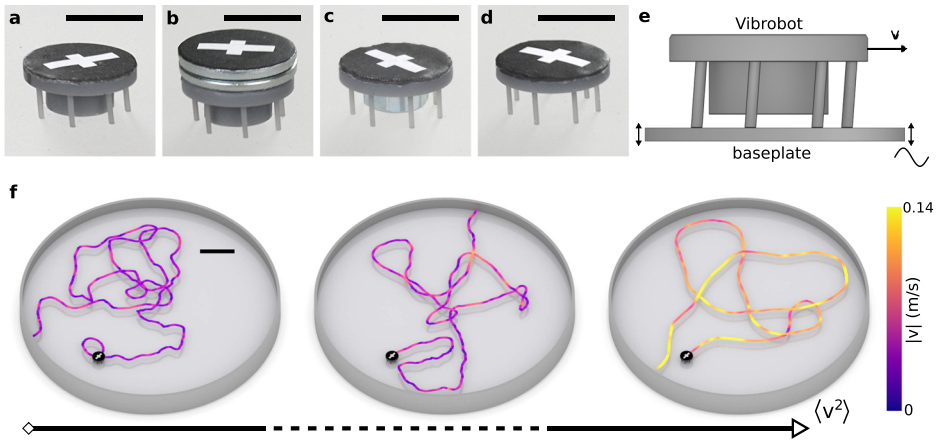

FIG. 5. 3D printed particles, setup, and trajectories. (a) *Generic particle*. (b) *Carrier particle* with an additional outer mass. (c) *Tug particle* with an additional central mass. (d) *Ring particle* without a central core. (e) Illustration of the mechanism with a generic particle on a vibrating plate. (f) Three exemplary trajectories with increasing average particle velocities. Particle images mark the starting point of each trajectory. The trajectory color indicates the magnitude of the velocity. Reproduced with permission from Scholz *et al.*, Nat. Commun. **9**, 5156 (2018). Copyright 2018 Author(s), licensed under a Creative Commons Attribution 4.0 License.

as the additional aligning torque described in Eq. (40) needs to be included. Moreover, there is no major difficulty in placing granulars on a turntable or on an oscillating plate so that effects arising from a noninertial frame are directly accessible. There is a plethora of other examples of macroscopic self-propelling objects, which are dominated by inertia. These include minirobots,[27,28] flying whirling fruits,[26] and walking droplets[92,93] as well as cars, boats, airplanes, swimming and flying animals,[32] and moving pedestrians, bicyclists, and vehicles.[94–97]

Regarding the second situation, dust particles in plasmas ("complex plasmas") can be made active.[98] They exhibit underdamped dynamics due to the presence of the neutral gas[10] and are, therefore, highly inertial. Another example in nature is fairyflies that belong to the smallest flying insects on our globe and have a size of several hundreds of micrometers.

B. Vibrated granulars in particular

As already mentioned, a direct realization of active Langevin motion is obtained for vibrated granulars. Interestingly, particles can be prepared with different mass and different moments of inertia (see Ref. 26), which we describe now in more detail. Exposed to a vibrating plate, they perform self-propulsion in two dimensions (see Fig. 5 for the experimental realization and typical particle trajectories). The actual particle velocity along the trajectories is not constant but fluctuates and the mean-square displacements and orientational correlations are in good agreement with the active Langevin model when some parameters are fitted to the experiments. In particular, the velocity distribution function has a peak around the self-propulsion velocity.

Interestingly, experimental data for the inertial delay as embodied in the delay correlation function $d(t)$ [see Eq. (18)] are both in qualitative and quantitative agreement with the theoretical result. An example is shown in Fig. 6. Indeed, the theoretical prediction is confirmed by the experimental data averaged over the noise. This demonstrates that first the direction of self-propulsion is changed and the velocity follows. As this delay effect is missing in the overdamped case, it must be caused completely by inertia. It is exactly this inertial delay effect that is used by oversteering racing cars to get around corners. We finally remark that, as compared to hexbugs, no self-aligning forces[23] need to be incorporated to get a reasonable fit of the data.

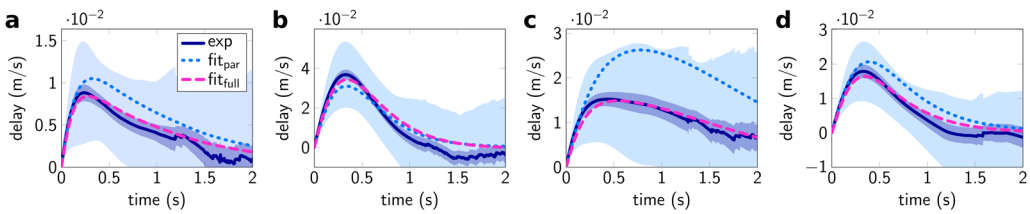

FIG. 6. Delay functions $d(t)$ for the (a) generic, (b) carrier, (c) tug, and (d) ring particle. The dark blue solid curve shows experimental data, the magenta dashed and light blue dotted curves plot theoretical results, with a different way of fitting. Experimental uncertainties are expressed as the standard deviation in light or dark blue regions. Reproduced with permission from Scholz *et al.*, Nat. Commun. **9**, 5156 (2018). Copyright 2018 Author(s), licensed under a Creative Commons Attribution 4.0 License.

VI. PERSPECTIVES

In the flourishing field of active matter, most of the investigations used simple overdamped dynamics such as active Brownian motion to model microswimmers and mesoscale self-propelled colloids. If it comes to more macroscopic active particles (granulars, hoppers, runners, or minirobots) or to motion in a gas ("microflyers"), inertial effects become relevant. Therefore, it is expected that future research will include more and more aspects of inertia also on a more fundamental level. In this article, we have mainly touched the basic model description of inertial active matter and their realization in granulate experiments.

Future activities and promising perspectives are expected along the following directions:

First, granulate particles will play a leading role as *paradigmatic realizations* for active matter models. Since they are macroscopic, the particles can more easily be manipulated and tailored. The particle shape can be easily changed by macroscopic 3D-printing and different particle interactions can be established. In detail:

(i) The whole field of *charged active matter* that unifies strongly coupled unscreened Coulomb systems[99] and active matter can be realized by charging granulars, by triboelectric effects, and by preparing macroscopic charged particles.[100] This is possibly a better controlled charged system than that of charged active dusty plasmas, which require nonequilibrium ionic fluxes.

(ii) Dipolar active particles with permanent magnetic dipole moments are not easy to synthesize on the colloidal level[101–104] but can directly be realized by equipping granular hoppers with little permanent magnets.

(iii) We are just beginning to study active polymers as colloidal chains. While there is an increasing number of simulation and theoretical studies (see Ref. 105 for a recent review), experimental studies with active polymers and colloidal chains in an active bath are sparse.[106] The effect of inertial dynamics on active polymers needs to be understood better, and future experiments and simulations are expected in this direction.

(iv) It would be highly interesting to study *active surfactants* to couple the field of surfactants with active matter. Chain-like vibrated granulars with a head and tail part composed of rotators with a different rotation sense[15,107] can be prepared and brought into motion to explore the dynamics at a surfactant interface.

(v) Studying granulars on a vibrating *structured substrate* will induce anisotropic active motion, which has not yet been studied by theory either.

(vi) Time-dependent propulsion strengths when the propulsion velocity depends explicitly on time can be realized by granulars, for example, by modulating the shaking amplitude on demand. For overdamped systems, some analytical results were obtained for time-dependent propulsions,[108] but inertia is expected to induce new lag-effects in the dynamics.[82]

Second, the motion of inertial active particles will be explored in various *confining geometries* (harmonic trap and confining walls). It has already been shown that in a simple harmonic confinement, there are novel dynamical effects.[23] This will be even more complex for more complicated confinements.

Third, *collective effects* of active Langevin dynamics need to be explored more. For instance, the impact of a nonvanishing moment of inertia and an external torque on MIPS should be studied. Moreover, the role of aligning interactions needs to be understood better for inertial systems.[66,109,110] Next, crystallization in active systems should be studied where inertia provides a latent heat upon crystallization (for a first study, see Ref. 111). In general, concerning collective effects, we do not only need benchmarking experiments but also fundamental theory including the Langevin dynamics. First attempts in terms of theory have been done by generalizing the swim pressure to the inertial case[73] and to consider inertial terms in hydrodynamic approaches[76,112] but certainly microscopic approaches such as mode-coupling theory[113,114] and dynamical density functional theory[115] also need to be extended to include inertia (see Ref. 116 for a recent approach). Next, active particles with inertia may provide little heat engines with a better efficiency than their overdamped counterparts as energy is not damped away by the dynamics. We are just at the beginning to understand the principles of entropy production (see, e.g., Refs. 117–119) and heat conversion[120–122] in these systems.

Finally, inertia introduces some kind of *memory* to the particle dynamics, both for translational and orientational motion, on the time scale of the inertial relaxation times τ and τ_r. This is the prime reason for delay effects relative to overdamped active Brownian particles. There is a need to classify memory effects, in general, and to study whether or not the behavior is similar to that in other systems governed by memory.[123,124] One other example where memory effects are crucial is an active particle in a viscoelastic (non-Newtonian) fluid such as a polymer solution[125] or a nematic liquid crystal[126,127] where a notable increase in the rotational diffusion coefficient has been found.[128] Another example is a sensorial delay in the perception of artificial minirobot systems,[27,28,129] which was shown to have a significant effect on the clustering and swarming properties.

VII. CONCLUSIONS

In conclusion, we have upgraded the standard model of active Brownian motion by including inertia in both translational and orientational motion leading to the basic model of active Langevin motion. We discussed single particle properties by the orientational and translational correlation functions presenting some analytical results for this model. When comparing the model to experiments on vibrated granulars, good agreement was found. We summarized some effects induced by inertia including an inertial delay between self-propulsion direction and particle velocity, the tuning of the long-time self-diffusion by the moment of inertia, the effect of fictitious forces in noninertial frames, and the influence of inertia on motility-induced phase separation. Since inertial effects will necessarily become relevant for length scales between macroscopic and mesoscopic both for artificial self-propelled objects and for living creatures, a booming future of inertial active systems is lying ahead.

ACKNOWLEDGMENTS

I thank Soudeh Jahanshahi, Christian Scholz, Thomas Franosch, Thomas Voigtmann, Alexander Sprenger, Alexei V. Ivlev, Frederik Hauke, and Suvendu Mandal for helpful discussions and gratefully acknowledge support from the Deutsche Forschungsgemeinschaft (DFG) through Grant No. LO 418/23-1.

REFERENCES

[1]T. Vicsek, A. Czirók, E. Ben-Jacob, I. Cohen, and O. Shochet, "Novel type of phase transition in a system of self-driven particles," Phys. Rev. Lett. **75**, 1226 (1995).
[2]J. R. Howse, R. A. Jones, A. J. Ryan, T. Gough, R. Vafabakhsh, and R. Golestanian, "Self-motile colloidal particles: From directed propulsion to random walk," Phys. Rev. Lett. **99**, 048102 (2007).
[3]B. ten Hagen, S. van Teeffelen, and H. Löwen, "Non-Gaussian behaviour of a self-propelled particle on a substrate," Condens. Matter Phys. **12**, 725–738 (2009).
[4]B. ten Hagen, S. van Teeffelen, and H. Löwen, "Brownian motion of a self-propelled particle," J. Phys.: Condens. Matter **23**, 194119 (2011).
[5]F. Kümmel, B. ten Hagen, R. Wittkowski, I. Buttinoni, R. Eichhorn, G. Volpe, H. Löwen, and C. Bechinger, "Circular motion of asymmetric self-propelling particles," Phys. Rev. Lett. **110**, 198302 (2013).
[6]C. Kurzthaler, C. Devailly, J. Arlt, T. Franosch, W. C. Poon, V. A. Martinez, and A. T. Brown, "Probing the spatiotemporal dynamics of catalytic Janus particles with single-particle tracking and differential dynamic microscopy," Phys. Rev. Lett. **121**, 078001 (2018).
[7]C. Bechinger, R. Di Leonardo, H. Löwen, C. Reichhardt, G. Volpe, and G. Volpe, "Active particles in complex and crowded environments," Rev. Mod. Phys. **88**, 045006 (2016).
[8]A. Fiasconaro, W. Ebeling, and E. Gudowska-Nowak, "Active Brownian motion models and applications to ratchets," Eur. Phys. J. B **65**, 403–414 (2008).
[9]P. Romanczuk, M. Bär, W. Ebeling, B. Lindner, and L. Schimansky-Geier, "Active Brownian particles: From individual to collective stochastic dynamics," Eur. Phys. J. Spec. Top. **202**, 1–162 (2012).
[10]G. E. Morfill and A. V. Ivlev, "Complex plasmas: An interdisciplinary research field," Rev. Mod. Phys. **81**, 1353 (2009).
[11]J. Bartnick, A. Kaiser, H. Löwen, and A. V. Ivlev, "Emerging activity in bilayered dispersions with wake-mediated interactions," J. Chem. Phys. **144**, 224901 (2016).
[12]A. Ivlev, J. Bartnick, M. Heinen, C.-R. Du, V. Nosenko, and H. Löwen, "Statistical mechanics where Newton's third law is broken," Phys. Rev. X **5**, 011035 (2015).
[13]V. Narayan, S. Ramaswamy, and N. Menon, "Long-lived giant number fluctuations in a swarming granular nematic," Science **317**, 105–108 (2007).
[14]C. A. Weber, T. Hanke, J. Deseigne, S. Léonard, O. Dauchot, E. Frey, and H. Chaté, "Long-range ordering of vibrated polar disks," Phys. Rev. Lett. **110**, 208001 (2013).
[15]C. Scholz, M. Engel, and T. Pöschel, "Rotating robots move collectively and self-organize," Nat. Commun. **9**, 931 (2018).
[16]A. Deblais, T. Barois, T. Guerin, P.-H. Delville, R. Vaudaine, J. S. Lintuvuori, J.-F. Boudet, J.-C. Baret, and H. Kellay, "Boundaries control collective dynamics of inertial self-propelled robots," Phys. Rev. Lett. **120**, 188002 (2018).
[17]A. Kudrolli, G. Lumay, D. Volfson, and L. S. Tsimring, "Swarming and swirling in self-propelled polar granular rods," Phys. Rev. Lett. **100**, 058001 (2008).
[18]J. Deseigne, O. Dauchot, and H. Chaté, "Collective motion of vibrated polar disks," Phys. Rev. Lett. **105**, 098001 (2010).
[19]G. A. Patterson, P. I. Fierens, F. S. Jimka, P. König, A. Garcimartín, I. Zuriguel, L. A. Pugnaloni, and D. R. Parisi, "Clogging transition of vibration-driven vehicles passing through constrictions," Phys. Rev. Lett. **119**, 248301 (2017).
[20]G. Junot, G. Briand, R. Ledesma-Alonso, and O. Dauchot, "Active versus passive hard disks against a membrane: Mechanical pressure and instability," Phys. Rev. Lett. **119**, 028002 (2017).
[21]G. Notomista, S. Mayya, A. Mazumdar, S. Hutchinson, and M. Egerstedt, "A study of a class of vibration-driven robots: Modeling, analysis, control and design of the brushbot," e-print arXiv:1902.10830 (2019).
[22]S. Mayya, G. Notomista, D. Shell, S. Hutchinson, and M. Egerstedt, "Achieving non-uniform densities in vibration driven robot swarms using phase separation theory," e-print arXiv:1902.10662 (2019).
[23]O. Dauchot and V. Démery, "Dynamics of a self-propelled particle in a harmonic trap," Phys. Rev. Lett. **122**, 068002 (2019).
[24]L. Walsh, C. G. Wagner, S. Schlossberg, C. Olson, A. Baskaran, and N. Menon, "Noise and diffusion of a vibrated self-propelled granular particle," Soft Matter **13**, 8964–8968 (2017).
[25]Y. Lanoiselée, G. Briand, O. Dauchot, and D. S. Grebenkov, "Statistical analysis of random trajectories of vibrated disks: Towards a macroscopic realization of Brownian motion," Phys. Rev. E **98**, 062112 (2018).
[26]C. Scholz, S. Jahanshahi, A. Ldov, and H. Löwen, "Inertial delay of self-propelled particles," Nat. Commun. **9**, 5156 (2018).
[27]M. Mijalkov and G. Volpe, "Sorting of chiral microswimmers," Soft Matter **9**, 6376–6381 (2013).
[28]M. Leyman, F. Ogemark, J. Wehr, and G. Volpe, "Tuning phototactic robots with sensorial delays," Phys. Rev. E **98**, 052606 (2018).
[29]D. Klotsa, "As above, so below, and also in between: Mesoscale active matter in fluids," Soft Matter **15**, 8946–8950 (2019).
[30]H. Mukundarajan, T. C. Bardon, D. H. Kim, and M. Prakash, "Surface tension dominates insect flight on fluid interfaces," J. Exp. Biol. **219**, 752–766 (2016).
[31]M. Turner, private communication (2019).
[32]J. Rabault, R. A. Fauli, and A. Carlson, "Curving to fly: Synthetic adaptation unveils optimal flight performance of whirling fruits," Phys. Rev. Lett. **122**, 024501 (2019).
[33]H. Löwen, "Chirality in microswimmer motion: From circle swimmers to active turbulence," Eur. Phys. J.: Spec. Top. **225**, 2319–2331 (2016).
[34]J.-P. Hansen and I. R. McDonald, *Theory of Simple Liquids* (Elsevier 1990).
[35]S. Mandal, L. Schrack, H. Löwen, M. Sperl, and T. Franosch, "Persistent anti-correlations in Brownian dynamics simulations of dense colloidal suspensions revealed by noise suppression," Phys. Rev. Lett. **123**, 168001 (2019).
[36]J. K. Dhont, *An Introduction to Dynamics of Colloids* (Elsevier, 1996), Vol. 2.
[37]X. Zheng, B. ten Hagen, A. Kaiser, M. Wu, H. Cui, Z. Silber-Li, and H. Löwen, "Non-Gaussian statistics for the motion of self-propelled Janus particles: Experiment versus theory," Phys. Rev. E **88**, 032304 (2013).
[38]S. van Teeffelen and H. Löwen, "Dynamics of a Brownian circle swimmer," Phys. Rev. E **78**, 020101 (2008).
[39]Y. Sumino, K. H. Nagai, Y. Shitaka, D. Tanaka, K. Yoshikawa, H. Chaté, and K. Oiwa, "Large-scale vortex lattice emerging from collectively moving microtubules," Nature **483**, 448 (2012).
[40]T. Sugi, H. Ito, M. Nishimura, and K. H. Nagai, "*C. elegans* collectively forms dynamical networks," Nat. Commun. **10**, 683 (2019).
[41]C. Chen, S. Liu, X.-q. Shi, H. Chaté, and Y. Wu, "Weak synchronization and large-scale collective oscillation in dense bacterial suspensions," Nature **542**, 210 (2017).
[42]A. Zöttl and H. Stark, "Emergent behavior in active colloids," J. Phys. Condens. Matter **28**, 253001 (2016).
[43]J. Bialké, T. Speck, and H. Löwen, "Crystallization in a dense suspension of self-propelled particles," Phys. Rev. Lett. **108**, 168301 (2012).
[44]P. Digregorio, D. Levis, A. Suma, L. F. Cugliandolo, G. Gonnella, and I. Pagonabarraga, "Full phase diagram of active Brownian disks: From melting to motility-induced phase separation," Phys. Rev. Lett. **121**, 098003 (2018).
[45]J. U. Klamser, S. C. Kapfer, and W. Krauth, "Thermodynamic phases in two-dimensional active matter," Nat. Commun. **9**, 5045 (2018).
[46]J. U. Klamser, S. C. Kapfer, and W. Krauth, "A kinetic-Monte Carlo perspective on active matter," J. Chem. Phys. **150**, 144113 (2019).
[47]H. H. Wensink, J. Dunkel, S. Heidenreich, K. Drescher, R. E. Goldstein, H. Löwen, and J. M. Yeomans, "Meso-scale turbulence in living fluids," Proc. Natl. Acad. Sci. U. S. A. **109**, 14308–14313 (2012).
[48]Y. Fily and M. C. Marchetti, "Athermal phase separation of self-propelled particles with no alignment," Phys. Rev. Lett. **108**, 235702 (2012).

[49]I. Buttinoni, J. Bialké, F. Kümmel, H. Löwen, C. Bechinger, and T. Speck, "Dynamical clustering and phase separation in suspensions of self-propelled colloidal particles," Phys. Rev. Lett. **110**, 238301 (2013).
[50]J. Palacci, S. Sacanna, A. P. Steinberg, D. J. Pine, and P. M. Chaikin, "Living crystals of light-activated colloidal surfers," Science **339**, 936–940 (2013).
[51]G. S. Redner, M. F. Hagan, and A. Baskaran, "Structure and dynamics of a phase-separating active colloidal fluid," Phys. Rev. Lett. **110**, 055701 (2013).
[52]Y. Fily, S. Henkes, and M. C. Marchetti, "Freezing and phase separation of self-propelled disks," Soft Matter **10**, 2132–2140 (2014).
[53]L. F. Cugliandolo, P. Digregorio, G. Gonnella, and A. Suma, "Phase coexistence in two-dimensional passive and active dumbbell systems," Phys. Rev. Lett. **119**, 268002 (2017).
[54]X.-q. Shi and H. Chaté, "Self-propelled rods: Linking alignment-dominated and repulsion-dominated active matter," e-print arXiv:1807.00294 (2018).
[55]A. P. Solon, J. Stenhammar, R. Wittkowski, M. Kardar, Y. Kafri, M. E. Cates, and J. Tailleur, "Pressure and phase equilibria in interacting active Brownian spheres," Phys. Rev. Lett. **114**, 198301 (2015).
[56]S. C. Takatori, W. Yan, and J. F. Brady, "Swim pressure: Stress generation in active matter," Phys. Rev. Lett. **113**, 028103 (2014).
[57]P. Krinninger, M. Schmidt, and J. M. Brader, "Nonequilibrium phase behavior from minimization of free power dissipation," Phys. Rev. Lett. **117**, 208003 (2016).
[58]J. Bialké, T. Speck, and H. Löwen, "Active colloidal suspensions: Clustering and phase behavior," J. Non-Cryst. Solids **407**, 367–375 (2015).
[59]M. E. Cates and J. Tailleur, "Motility-induced phase separation," Annu. Rev. Condens. Matter Phys. **6**, 219–244 (2015).
[60]G. Gonnella, D. Marenduzzo, A. Suma, and A. Tiribocchi, "Motility-induced phase separation and coarsening in active matter," C. R. Phys. **16**, 316–331 (2015).
[61]M. C. Marchetti, Y. Fily, S. Henkes, A. Patch, and D. Yllanes, "Minimal model of active colloids highlights the role of mechanical interactions in controlling the emergent behavior of active matter," Curr. Opin. Colloid Interface Sci. **21**, 34–43 (2016).
[62]G.-J. Liao and S. H. Klapp, "Clustering and phase separation of circle swimmers dispersed in a monolayer," Soft Matter **14**, 7873–7882 (2018).
[63]B. Liebchen and D. Levis, "Collective behavior of chiral active matter: Pattern formation and enhanced flocking," Phys. Rev. Lett. **119**, 058002 (2017).
[64]D. Levis and B. Liebchen, "Simultaneous phase separation and pattern formation in chiral active mixtures," Phys. Rev. E **100**, 012406 (2019).
[65]Q.-L. Lei, M. P. Ciamarra, and R. Ni, "Nonequilibrium strongly hyperuniform fluids of circle active particles with large local density fluctuations," Science Adv. **5**, eaau7423 (2019).
[66]E. Sese-Sansa, I. Pagonabarraga, and D. Levis, "Velocity alignment promotes motility-induced phase separation," Europhys. Lett. **124**, 30004 (2018).
[67]M. Theers, E. Westphal, K. Qi, R. G. Winkler, and G. Gompper, "Clustering of microswimmers: Interplay of shape and hydrodynamics," Soft Matter **14**, 8590–8603 (2018).
[68]M. N. van der Linden, L. C. Alexander, D. G. A. L. Aarts, and O. Dauchot, "Interrupted motility induced phase separation in aligning active colloids," Phys. Rev. Lett. **123**, 098001 (2019).
[69]J. Stenhammar, A. Tiribocchi, R. J. Allen, D. Marenduzzo, and M. E. Cates, "Continuum theory of phase separation kinetics for active Brownian particles," Phys. Rev. Lett. **111**, 145702 (2013).
[70]T. Speck, J. Bialké, A. M. Menzel, and H. Löwen, "Effective Cahn-Hilliard equation for the phase separation of active Brownian particles," Phys. Rev. Lett. **112**, 218304 (2014).
[71]A. Baskaran and M. C. Marchetti, "Enhanced diffusion and ordering of self-propelled rods," Phys. Rev. Lett. **101**, 268101 (2008).
[72]M. Enculescu and H. Stark, "Active colloidal suspensions exhibit polar order under gravity," Phys. Rev. Lett. **107**, 058301 (2011).
[73]S. C. Takatori and J. F. Brady, "Inertial effects on the stress generation of active fluids," Phys. Rev. Fluids **2**, 094305 (2017).
[74]Z. Mokhtari, T. Aspelmeier, and A. Zippelius, "Collective rotations of active particles interacting with obstacles," Europhys. Lett. **120**, 14001 (2017).
[75]S. Shankar and M. C. Marchetti, "Hidden entropy production and work fluctuations in an ideal active gas," Phys. Rev. E **98**, 020604 (2018).
[76]A. Manacorda and A. Puglisi, "Lattice model to derive the fluctuating hydrodynamics of active particles with inertia," Phys. Rev. Lett. **119**, 208003 (2017).
[77]S. Das, G. Gompper, and R. G. Winkler, "Local stress and pressure in an inhomogeneous system of spherical active Brownian particles," Sci. Rep. **9**, 6608 (2019).
[78]H. D. Vuijk, J.-U. Sommer, H. Merlitz, J. M. Brader, and A. Sharma, "Lorentz forces induce inhomogeneity and fluxes in active systems," e-print arXiv:1908.02577 (2019).
[79]I. Abdoli, H. D. Vuijk, J.-U. Sommer, J. M. Brader, and A. Sharma, "Nondiffusive fluxes in Brownian system with Lorentz force," e-print arXiv:1908.03101 (2019).
[80]J. Um, T. Song, and J.-H. Jeon, "Langevin dynamics driven by a telegraphic active noise," Front. Phys. **7**, 143 (2019).
[81]P. K. Ghosh, Y. Li, G. Marchegiani, and F. Marchesoni, "Communication: Memory effects and active Brownian diffusion," J. Chem. Phys. **143**, 211101 (2015).
[82]S. Jahanshahi, "Microswimmers and microflyers in various complex environments," Ph.D. thesis, HHU Düsseldorf, 2019; see docserv.uni-duesseldorf.de.
[83]K. Malakar, A. Das, A. Kundu, K. V. Kumar, and A. Dhar, "Exact steady state of active Brownian particles in a 2d harmonic trap," e-print arXiv:1902.04171 (2019).
[84]C. Kurzthaler, S. Leitmann, and T. Franosch, "Intermediate scattering function of an anisotropic active Brownian particle," Sci. Rep. **6**, 36702 (2016).
[85]C. Kurzthaler and T. Franosch, "Intermediate scattering function of an anisotropic Brownian circle swimmer," Soft Matter **13**, 6396–6406 (2017).
[86]J. Deseigne, S. Leonard, O. Dauchot, and H. Chate, "Vibrated polar disks: spontaneous motion, binary collisions, and collective dynamics," Soft Matter **8**, 5629–5639 (2012).
[87]H. Löwen, "Active particles in noninertial frames: How to self-propel on a carousel," Phys. Rev. E **99**, 062608 (2019).
[88]A. Suma, G. Gonnella, D. Marenduzzo, and E. Orlandini, "Motility-induced phase separation in an active dumbbell fluid," Europhys. Lett. **108**, 56004 (2014).
[89]S. Mandal, B. Liebchen, and H. Löwen, "Motility-induced temperature difference in coexisting phases," Phys. Rev. Lett. **123**, 228001 (2019).
[90]I. Petrelli, P. Digregorio, L. F. Cugliandolo, G. Gonnella, and A. Suma, "Active dumbbells: Dynamics and morphology in the coexisting region," Eur. Phys. J. E **41**, 128 (2018).
[91]Y. Komatsu and H. Tanaka, "Roles of energy dissipation in a liquid-solid transition of out-of-equilibrium systems," Phys. Rev. X **5**, 031025 (2015).
[92]Y. Couder and E. Fort, "Single-particle diffraction and interference at a macroscopic scale," Phys. Rev. Lett. **97**, 154101 (2006).
[93]R. N. Valani, A. C. Slim, and T. Simula, "Superwalking droplets," Phys. Rev. Lett. **123**, 024503 (2019).
[94]D. Helbing, "Traffic and related self-driven many-particle systems," Rev. Mod. Phys. **73**, 1067 (2001).
[95]J. Zhang, W. Mehner, E. Andresen, S. Holl, M. Boltes, A. Schadschneider, and A. Seyfried, "Comparative analysis of pedestrian, bicycle and car traffic moving in circuits," Procedia **104**, 1130–1138 (2013).
[96]D. Chowdhury, L. Santen, and A. Schadschneider, "Statistical physics of vehicular traffic and some related systems," Phys. Rep. **329**, 199–329 (2000).
[97]A. Nakayama, M. Kikuchi, A. Shibata, Y. Sugiyama, S.-i. Tadaki, and S. Yukawa, "Quantitative explanation of circuit experiments and real traffic using the optimal velocity model," New J. Phys. **18**, 043040 (2016).
[98]J. Bartnick, M. Heinen, A. V. Ivlev, and H. Löwen, "Structural correlations in diffusiophoretic colloidal mixtures with nonreciprocal interactions," J. Phys. Condens. Matt. **28**, 025102 (2016).
[99]Y. Levin, "Electrostatic correlations: From plasma to biology," Rep. Prog. Phys. **65**, 1577 (2002).
[100]J. Haeberle, J. Harju, M. Sperl, and P. Born, "Granular ionic crystals in a small nutshell," Soft Matter **15**, 7179–7186 (2019).
[101]N. Casic, N. Quintero, R. Alvarez-Nodarse, F. G. Mertens, L. Jibuti, W. Zimmermann, and T. M. Fischer, "Propulsion efficiency of a dynamic self-assembled helical ribbon," Phys. Rev. Lett. **110**, 168302 (2013).

[102]G. Steinbach, S. Gemming, and A. Erbe, "Non-equilibrium dynamics of magnetically anisotropic particles under oscillating fields," Eur. Phys. J. E **39**, 69 (2016).
[103]A. Nourhani, D. Brown, N. Pletzer, and J. G. Gibbs, "Engineering contactless particle–particle interactions in active microswimmers," Adv. Mater. **29**, 1703910 (2017).
[104]G. Grosjean, M. Hubert, Y. Collard, A. Sukhov, J. Harting, A.-S. Smith, and N. Vandewalle, "Capillary assemblies in a rotating magnetic field," Soft Matter **15**, 9093–9103 (2019).
[105]R. G. Winkler, J. Elgeti, and G. Gompper, "Active polymers—Emergent conformational and dynamical properties: A brief review," J. Phys. Soc. Jpn. **86**, 101014 (2017).
[106]J. Yan, M. Han, J. Zhang, C. Xu, E. Luijten, and S. Granick, "Reconfiguring active particles by electrostatic imbalance," Nat. Mater. **15**, 1095 (2016).
[107]N. H. P. Nguyen, D. Klotsa, M. Engel, and S. C. Glotzer, "Emergent collective phenomena in a mixture of hard shapes through active rotation," Phys. Rev. Lett. **112**, 075701 (2014).
[108]S. Babel, B. ten Hagen, and H. Löwen, "Swimming path statistics of an active Brownian particle with time-dependent self-propulsion," J. Stat. Mech. Theor. Exp. **2014**, P02011.
[109]P. Degond, S. Henkes, and H. Yu, "Self-organized hydrodynamics with density-dependent velocity," Kinet. Relat. Models **10**, 193–213 (2017).
[110]R. van Damme, J. Rodenburg, R. van Roij, and M. Dijkstra, "Interparticle torques suppress motility-induced phase separation for rodlike particles," J. Chem. Phys. **150**, 164501 (2019).
[111]G. Briand, M. Schindler, and O. Dauchot, "Spontaneously flowing crystal of self-propelled particles," Phys. Rev. Lett. **120**, 208001 (2018).
[112]R. Chatterjee, N. Rana, R. A. Simha, P. Perlekar, and S. Ramaswamy, "Fluid flocks with inertia," e-print arXiv:1907.03492 (2019).
[113]A. Liluashvili, J. Ónody, and T. Voigtmann, "Mode-coupling theory for active Brownian particles," Phys. Rev. E **96**, 062608 (2017).
[114]G. Szamel, "Mode-coupling theory for the steady-state dynamics of active Brownian particles," J. Chem. Phys. **150**, 124901 (2019).
[115]A. M. Menzel, A. Saha, C. Hoell, and H. Löwen, "Dynamical density functional theory for microswimmers," J. Chem. Phys. **144**, 024115 (2016).
[116]D. Arold and M. Schmiedeberg, "Mean field approach of dynamical pattern formation in underdamped active matter with short-ranged alignment and distant anti-alignment interactions," e-print arXiv:1912.07038 (2019).
[117]C. Nardini, É. Fodor, E. Tjhung, F. van Wijland, J. Tailleur, and M. E. Cates, "Entropy production in field theories without time-reversal symmetry: quantifying the non-equilibrium character of active matter," Phys. Rev. X **7**, 021007 (2017).
[118]P. Pietzonka and U. Seifert, "Entropy production of active particles and for particles in active baths," J. Phys. A **51**, 01LT01 (2017).
[119]S. Chaki and R. Chakrabarti, "Entropy production and work fluctuation relations for a single particle in active bath," Physica A **511**, 302–315 (2018).
[120]S. Krishnamurthy, S. Ghosh, D. Chatterji, R. Ganapathy, and A. Sood, "A micrometre-sized heat engine operating between bacterial reservoirs," Nat. Phys. **12**, 1134 (2016).
[121]D. Martin, C. Nardini, M. E. Cates, and É. Fodor, "Extracting maximum power from active colloidal heat engines," Europhys. Lett. **121**, 60005 (2018).
[122]K. Brandner, K. Saito, and U. Seifert, "Thermodynamics of micro-and nano-systems driven by periodic temperature variations," Phys. Rev. X **5**, 031019 (2015).
[123]H. Meyer, P. Pelagejcev, and T. Schilling, "Non-Markovian out-of-equilibrium dynamics: A general numerical procedure to construct time-dependent memory kernels for coarse-grained observables," e-print arXiv:1905.11753 (2019).
[124]K. H. Nagai, Y. Sumino, R. Montagne, I. S. Aranson, and H. Chaté, "Collective motion of self-propelled particles with memory," Phys. Rev. Lett. **114**, 168001 (2015).
[125]J. Berner, B. Müller, J. R. Gomez-Solano, M. Krüger, and C. Bechinger, "Oscillating modes of driven colloids in overdamped systems," Nat. Commun. **9**, 999 (2018).
[126]J. Toner, H. Löwen, and H. H. Wensink, "Following fluctuating signs: Anomalous active superdiffusion of swimmers in anisotropic media," Phys. Rev. E **93**, 062610 (2016).
[127]A. Daddi-Moussa-Ider and A. M. Menzel, "Dynamics of a simple model microswimmer in an anisotropic fluid: Implications for alignment behavior and active transport in a nematic liquid crystal," Phys. Rev. Fluids **3**, 094102 (2018).
[128]J. R. Gomez-Solano, A. Blokhuis, and C. Bechinger, "Dynamics of self-propelled Janus particles in viscoelastic fluids," Phys. Rev. Lett. **116**, 138301 (2016).
[129]R. Piwowarczyk, M. Selin, T. Ihle, and G. Volpe, "Influence of sensorial delay on clustering and swarming," Phys. Rev. E **100**, 012607 (2019).